

Wang-Landau simulation for the quasi-one-dimensional Ising model

Takayuki TANABE¹ and Kouichi OKUNISHI²

¹Graduate School of Science, Niigata University, Igarashi 2, 8050 Niigata 950-2181, Japan.

²Department of Physics, Faculty of Science, Niigata University, Igarashi 2, 8050 Niigata 950-2181, Japan.

We revisit the nature of the quasi-one-dimensional Ising model on the basis of Wang-Landau simulation. We introduce the density of states in the two dimensional energy space corresponding to the intra- and inter-chain directions. We then analyze the inter-chain coupling dependence of the specific heat of the anisotropic 2D Ising model in the context of the density of states, and further discuss the size dependences of the peak temperature. We also discuss the feature of the phase transition for 3D case.

KEYWORDS: quasi-one-dimension, Wang-Landau simulation, density of states

1. Introduction

Effect of the inter-chain coupling in the quasi-one-dimensional(Q1D) spin systems has been attracting much attention. In general, the 1D spin system shows no phase transition at a finite temperature. In the Q1D system, however, the weak inter-chain coupling induces a finite temperature phase transition. In fact, the 3D long range ordering for the Q1D system has been a long standing issue.¹ The recent experimental developments enable precise investigation of 3D ordering in a wide variety of the Q1D systems, such as coupled $S = 1/2$ Heisenberg chains.² Very recently, moreover, it was shown that the Q1D Ising-like XXZ antiferromagnet $\text{BaCu}_2\text{V}_2\text{O}_8$ exhibits the exotic incommensurate spin order in the magnetic field,^{3,4} for which the Ising anisotropy plays an essential role.

Motivated the experimental results above, we reexamine the phase transition of the Q1D Ising system:

$$\mathcal{H} = -J \sum_{\langle i,j \rangle_{\parallel}} S_i S_j - J' \sum_{\langle i,j \rangle_{\perp}} S_i S_j \quad (1)$$

where $S \in \pm 1$ is the Ising spin variable, $\langle i, j \rangle_{\parallel}$ indicates spin pairs along the chain direction, and $\langle i, j \rangle_{\perp}$ means the pairs perpendicular to the chain. Thus J and J' respectively represent the coupling constants for the intra-chain and inter-chain interactions. Of course the universality of the Ising transition due to the Z_2 symmetry breaking itself is independent of the inter-chain interaction. However, the quantitative details of the inter-chain dependence of the phase transition still involves an interesting problem,⁵⁻⁸ which is essential to resolve experimental results. Recently the universal reduction of the effective coordination number is also reported for the Q1D Ising model.⁹ The aim of this paper is to understand the role of the inter-chain coupling in the context of the energy density of states(DOS) based on Wang-Landau simulation^{11,12} and then we discuss the size dependence of the transition temperature of the Q1D Ising system.

For the quantitative analysis of such a phase transition of the Q1D system, we should recall that the energy scale of the inter-chain coupling is much smaller than that of intra-chain coupling and thus the transition temperature becomes very low; the conventional metropolis

Monte Carlo simulation based on local spin flip often fails relaxation to the proper equilibrium state. Recently an efficient cluster algorithm is proposed for the Q1D system.¹⁰ In this paper, however, we employ the Wang-Landau simulation, which enable for us to estimate the DOS through the random walk in the energy space and to avoid trapping to a metastable state.^{11,12} This is because, on the basis of the DOS, we can resolve the contribution from the typical configurations at low temperature, which provides an essential view point of the low temperature behavior of the Q1D system.

This paper is organized as follows. In the next section, we briefly explain details of the Wang-Landau simulation for the Q1D system. In particular we introduce DOS of two dimensional energy space for the intra-chain and inter-chain directions. In §3, we discuss the phase transition for the 2D case in the context of DOS and then analyze the inter-chain interaction dependence of the phase transition. For 3D case, we also discuss the nature of the phase transition. In §4 conclusion is summarized.

2. Simulation details

The Wang-Landau simulation is based on the random walk in the energy space without trapping metastable state and enables for us to estimate DOS. For the Q1D system, however, the energy scale of the inter-chain coupling is fairly different from the intra-chain coupling. For the purpose of treating such a highly anisotropic system more efficiently, we further introduce the two dimensional energy space defined by

$$e_{\parallel} \equiv \sum_{\langle i,j \rangle_{\parallel}} S_i S_j, \quad \text{and} \quad e_{\perp} \equiv \sum_{\langle i,j \rangle_{\perp}} S_i S_j. \quad (2)$$

where e_{\parallel} and e_{\perp} mean (dimensionless) unbiased energy for the intra-chain direction and inter-chain direction. Then the total energy is given by $E = -J e_{\parallel} - J' e_{\perp}$. The Wang-Landau simulation itself is performed for *this two dimensional space of the spatially isotropic Ising model* and then obtain DOS $g(e_{\parallel}, e_{\perp})$ in $(e_{\parallel}, e_{\perp})$ space. The expectation value for various J' can be obtained through reweighting.

The detailed conditions for the Wang-Landau simulation was given as the followings. At the start of a simulation, DOS is unknown, so it is simply set $g(e_{\parallel}, e_{\perp}) =$

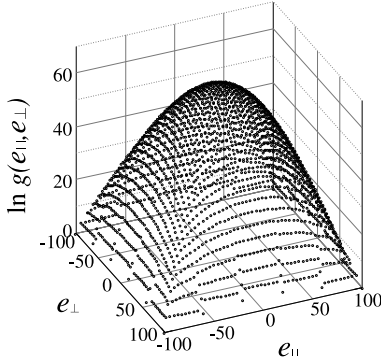


Fig. 1. Two dimensional DOS of the 2D Ising model of the system size $L=10$

1 for all possible $(e_{||}, e_{\perp})$. Then we begin a random walk in $(e_{||}, e_{\perp})$ space with a probability proportional to $1/g(e_{||}, e_{\perp})$. The transition probability from $(e'_{||}, e'_{\perp})$ to $(e''_{||}, e''_{\perp})$ is

$$\text{Prob}((e'_{||}, e'_{\perp}) \rightarrow (e''_{||}, e''_{\perp})) = \min \left[\frac{g(e'_{||}, e'_{\perp})}{g(e''_{||}, e''_{\perp})}, 1 \right], \quad (3)$$

and $g(e_{||}, e_{\perp})$ is iteratively updated by a modification factor f as

$$\ln g(e_{||}, e_{\perp}) \rightarrow \ln g(e_{||}, e_{\perp}) + \ln f, \quad (4)$$

when the state is visited. At the same time, the histogram is updated like $H(e_{||}, e_{\perp}) \rightarrow H(e_{||}, e_{\perp}) + 1$. When the histogram becomes "flat", the modification factor is reduced $\ln f \rightarrow (\ln f)/2$ and we reset the histogram to zero. Then we perform random walk again. To check the flatness of the histogram, we use the criterion $(H_{\max} - H_{\min})/(H_{\max} + H_{\min}) \leq 0.1 \sim 0.3$, where H_{\max} and H_{\min} are the maximum and minimum histogram counts respectively.¹³ We end the simulation when the modification factor is smaller than a predefined value (we set $\ln f_{\text{final}} = 10^{-6}$). The initial value of the modification factor is $\ln f_0 = 1$. The update of $g(e_{||}, e_{\perp})$ and $H(e_{||}, e_{\perp})$ is performed every N spin flip, where N is the number of the spins in the system.¹⁴

3. Results

3.1 2D Ising model

Let us first consider the 2D Ising model on the $L \times L$ square lattice, the exact solution of which is well known¹⁵ and very useful to verify the simulation results. The Hamiltonian of the 2D Ising model is written as

$$\mathcal{H} = -J \sum_{i,j}^L S_{i,j} S_{i+1,j} - J' \sum_{i,j}^L S_{i,j} S_{i,j+1} \quad (5)$$

where i and j are indexes of the intra- and inter-chain directions respectively. The unbiased energies for the intra- and inter-chain directions are explicitly given by $e_{||} = \sum_{i,j}^L S_{i,j} S_{i+1,j}$ and $e_{\perp} = \sum_{i,j}^L S_{i,j} S_{i,j+1}$. Since $g(e_{||}, e_{\perp}) = g(-e_{||}, e_{\perp}) = g(e_{||}, -e_{\perp}) = g(-e_{||}, -e_{\perp})$ is hold, it is sufficient to perform simulation in the region $e_{||} \geq 0, e_{\perp} \geq 0$. The system sizes are $L = 10, 20, 30, 40$, and 50. The max histogram count per stage is $H_{\max} =$

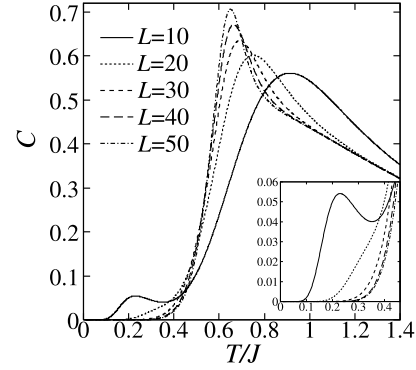


Fig. 2. Specific heat for $J'/J = 0.025$. Inset: magnification of the low temperature peak.

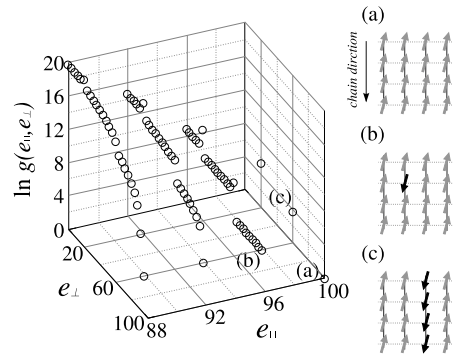


Fig. 3. Two dimensional DOS of the 2D Ising model of $L = 10$ near the groundstate ($88 \leq e_{||} \leq 100, 0 \leq e_{\perp} \leq 100$). The figures in the right panel indicate the configurations for (a) the ground state, (b) single spin flipped state, and (c) chain flipped state

3024, and the max Monte Carlo steps per stage is 1.7×10^8 for $L = 10$ system. Then the total stage number is 21, and the total CPU time is 2 minutes with a 2.66GHz Core2Duo processor. For $L = 30$, $H_{\max} = 7981$, the max Monte Carlo steps per stage is 3.3×10^{11} . The total stage number is also 21 and the total CPU time is 55 hours. In Fig. 1, we show the typical result of DOS $g(e_{||}, e_{\perp})$ for $L = 10$.

On the basis of DOS $g(e_{||}, e_{\perp})$, we calculate the specific heat; Figure 2 shows the size dependence of the specific heat for $J'/J = 0.025$. According to the exact solution of the 2D Ising model, the transition temperature for $J'/J = 0.025$ is given by $T_c/J = 0.6221 \dots$. The result clearly shows that the peak of C corresponding to the critical divergence gradually develops for $L = 50$ in the vicinity of T_c . In addition to the critical point, we can also see the small peak at the low temperature region $T/J \sim 0.2$. As L increases, the peak temperature of this small peak shifts to the higher temperature side and the peak height itself reduces rapidly.

In order to see the origin of the low temperature peak, we show the DOS $g(e_{||}, e_{\perp})$ in low energy region in Fig. 3. Note that the scale of $e_{||}$ is much smaller than e_{\perp} ; Since $J' \ll J$ for the Q1D system, the range of the horizontal axis in Fig.3 is adjusted by the ratio: $e_{||}/e_{\perp} \sim J'/J = 1/40$. The ground state energy is

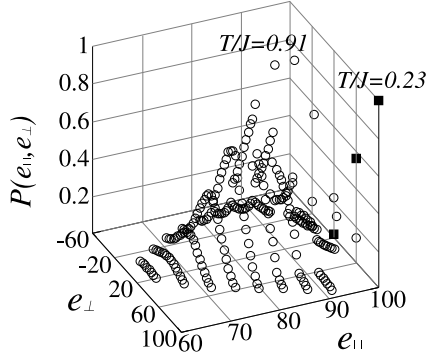


Fig. 4. Canonical distribution function for $J'/J = 0.025$ with $L = 10$. The solid squares indicate the distribution function for $T/J = 0.23$, which corresponds to the low temperature peak of the specific heat. The open circles indicate that for the high temperature peak ($T/J = 0.91$). Each distribution function is normalized so that the maximum value corresponds to unity.

$E_g = -(J + J')L \times L$ and its configuration is illustrated as Fig. 3(a), which is located at $(e_{||}, e_{\perp}) = (100, 100)$. As a low energy excitation, we usually consider the single spin flipped state given by Fig. 3(b), whose energy is $E_{(b)} = E_g + 4(J + J')$. For Q1D system, however, another important excitation we should discuss is “chain flipped excitation”, a typical example of which is depicted in Fig. 3(c), and its energy is given by $E_{(c)} = E_g + 4J'L$. The DOS of the chain flipped configuration is located at $e_{\perp} = 60, 20 \dots$ on the edge of $e_{||} = 100$. In Fig. 1, we can also confirm that the DOS of these configurations deviate at the edges $g(e_{||}, e_{\perp})$ plane. Moreover, note that “gap” in DOS at every $e_{\perp} = 20$ in Fig. 3 is also originating from the chain structure of the lattice. Since $L < J/J'$, we can see that the chain flipped excitation has a lower energy than the single spin flipped state and then it becomes the dominant excitation at a low temperature. As L increases beyond J/J' , the energy of the chain flipped excitations shifts to the higher energy region, so that the contribution from such configurations reduces gradually. Thus the low temperature peak of the specific heat in Fig. 2 can be well described by the chain flipped excitations, which is peculiar to the Q1D system.

In order to see the weight of each energy state in the equilibrium, we calculate the canonical distribution function

$$P(e_{||}, e_{\perp}) = g(e_{||}, e_{\perp}) \exp[-(J e_{||} + J' e_{\perp})/T] \quad (6)$$

for $J'/J = 0.025$, which is shown in Fig.4. Note that $T/J = 0.23$ is the temperature of the low temperature peak of the specific heat and $T/J = 0.91$ corresponds to the high temperature peak of $L = 10$. In the figure, the dominant contribution at $T/J = 0.23$ clearly comes from the states at the edge of $e_{\perp} = 100$, which implies that the chain flipped state is essential for the small peak; For the relatively small system size ($L < J/J'$), the energy of the excitations actually satisfies $4(J + J') > 4J'L$. On the other hand, the $P(e_{||}, e_{\perp})$ for $T/J = 0.91$ shows Gaussian like shape around $(e_{||}, e_{\perp}) \sim (90, 20)$, where the chain flipped state gives only minor contribution in DOS.

As mentioned above, the dominant contribution to the

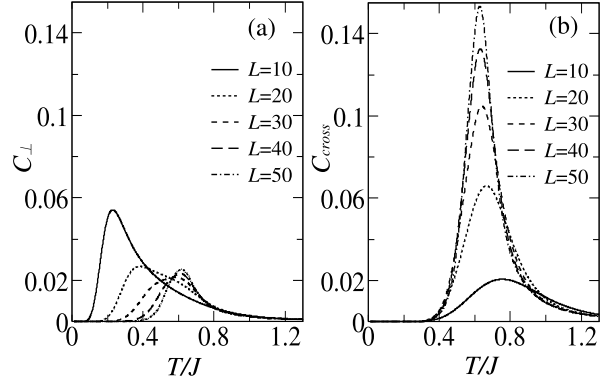


Fig. 5. The decomposed specific heats for $J'/J = 0.025$. (a) the energy fluctuation in the chain direction C_{\perp} , and the cross term of the chain and inter-chain directions C_{cross} .

low temperature peak ($T/J = 0.229$) is the chain flipped states near the ground state. This implies that the polarization of the spins in the same chain is basically frozen and the aligned spins of the chain can behave as a single spin, which forms an effective 1D spin chain through the weak inter-chain coupling LJ' in the inter-chain direction. Thus we can see that the fluctuation in the inter-chain direction is dominant for the low temperature peak, while at the high temperature peak, the fluctuations in both the intra- and inter-chain directions give the significant contributions. Of course, the low temperature peak is basically a finite size effect and it vanishes in the bulk limit. However the region where finite size effect can clearly appear is up to $L \sim J/J'$, which is a certain large number for the Q1D system. This implies that the true critical divergence of the specific heat is eventually masked by the analytic contribution originating from the low temperature peak, up to $L \sim J/J'$. Thus the finite size scaling analysis based on the data $L < J/J'$ should be performed carefully.¹⁷

In order to extract the proper critical behavior for $L < J/J'$, we examine the decomposition of the specific heat into three parts: the fluctuation along the chain $C_{||}$, the fluctuation in the inter-chain directions C_{\perp} and cross term of the intra- and inter-chain directions C_{cross} .

$$\begin{aligned} C &= (\langle E \rangle^2 - \langle E^2 \rangle) / NT^2 \\ &= C_{||} + C_{\perp} + C_{\text{cross}}, \end{aligned} \quad (7)$$

$$C_{||} = J^2 (\langle e_{||}^2 \rangle - \langle e_{||} \rangle^2) / NT^2, \quad (8)$$

$$C_{\perp} = J'^2 (\langle e_{\perp}^2 \rangle - \langle e_{\perp} \rangle^2) / NT^2, \quad (9)$$

$$C_{\text{cross}} = 2JJ' (\langle e_{||} e_{\perp} \rangle - \langle e_{||} \rangle \langle e_{\perp} \rangle) / NT^2. \quad (10)$$

In Fig. 5, we show C_{\perp} and C_{cross} for $J'/J = 0.025$ ($C_{||}$ is not presented here). In the figure, C_{\perp} shows the shot-key like peak for small system sizes ($L < 20$). As L increases, the peak position shifts to the high temperature side and the peak height itself rapidly reduces. This behavior is consistent with that the inter-chain fluctuation is the dominant contribution for $L < J/J'$. Indeed, we have verified that the low temperature peak of $L = 10$

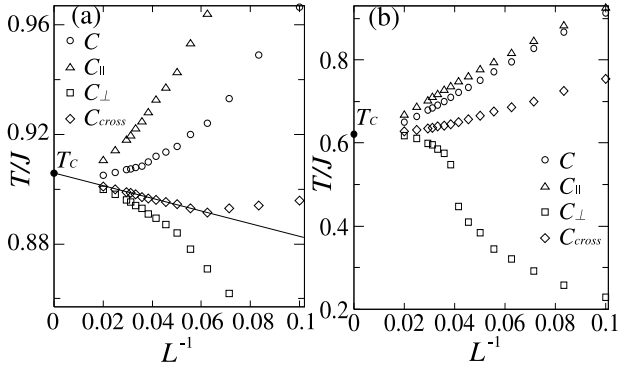


Fig. 6. The size dependences of the peak temperatures for C , $C_{||}$, C_{\perp} , and C_{cross} : (a) $J'/J = 0.1$ and (b) $J'/J = 0.025$. The solid circles at the vertical axis indicate the exact transition temperatures

can be well fitted by the specific heat of the 1D Ising chain of the effective coupling LJ' with $L = 10$. In addition to the low temperature peak, we can also see that a broad peak emerges around $T/J \sim 0.6$ as L increases; this peak corresponds to the critical divergence in the bulk limit. Thus the crossover of C_{\perp} from the effective 1D Ising model behavior to the 2D Ising model clearly appears around $L \sim J/J'$. On the other hand, the cross term C_{cross} shows the divergence behavior only near the correct critical temperature $T_c = 0.622 \dots$. This suggests that C_{cross} may capture the critical behavior more effectively than the total specific heat C .

We further analyze size dependence of the peak temperatures of decomposed specific heats C , $C_{||}$, C_{\perp} and C_{cross} . Let us write the peak temperature for the system size L as $T_c(L)$. Then, in the critical regime, the peak temperature is expected to follow the size scaling,

$$T_c(L) - T_c = AL^{-1/\nu} \quad (11)$$

where A is a nonuniversal constant. First we discuss the result for $J'/J = 0.1$, which are illustrated in Fig 6(a). In the figure we can see that C , $C_{||}$ and C_{\perp} gradually approach T_c , for which the scaling behavior is not still observed. However the cross term of the specific heat C_{cross} well satisfies (11) within relatively small system size ($1/L < 0.06$), suggesting that C_{cross} is rather effective to capture the critical behavior than C . Another interesting feature for the Q1D system is that $T_c(L)$ approaches T_c from the under side of T_c , namely $A > 0$, for sufficiently large L . This behavior is contrasted to $A < 0$ for the isotropic case where the peak temperatures of the all C s monotonously approach T_c from $T > T_c$.

The peak temperatures for $J'/J = 0.025$, which are shown in Fig.6(b), demonstrate a more typical size dependences of the Q1D system; The peak of $C_{||}$ monotonously decreases from the upper side of T_c , while C_{\perp} clearly exhibits the crossover behavior. For small $L (< 0.04)$, the peak position of C_{\perp} originates from the chain flip configuration. However we can see that it

rapidly crossovers to that of the critical behavior around $1/L \sim 0.04$. On the other hand, C_{cross} seems to approach T_c smoothly, suggesting that C_{cross} is more suitable for finite size analysis of the critical behavior. For $J'/J = 0.025$, however, we should note that system size may be still insufficient for the precise verification of the critical exponent ν .

3.2 3D Ising model

Let us discuss the 3D Ising model in the same line of argument as the 2D case. The Hamiltonian is written as

$$\begin{aligned} \mathcal{H} = & -J \sum_{i,j,k}^L S_{i,j,k} S_{i,j,k+1} \\ & - J' \sum_{i,j,k}^L [S_{i,j,k} S_{i+1,j,k} + S_{i,j,k} S_{i,j+1,k}] \quad (12) \end{aligned}$$

where k is assumed to run in the chain direction. In actual computations, the max histogram count per stage is $H_{\text{max}} = 6024$, and the max Monte Carlo steps per stage is 6.5×10^9 for $L = 6$ system. The total stage number is 21 and the total CPU time is 50 minutes. For $L = 10$, $H_{\text{max}} = 6748$, the max Monte Carlo steps per stage is 7.5×10^{11} , and the total CPU time is about 6 days. Here we note that, for 3D Ising model, Wang-Landau simulation in the 2D energy space (2) sometimes does not achieve well convergence near the edges of the 2D energy space. For such a case, we have supplementary performed Wang-Landau simulation for the conventional 1D energy space.

Figure 7(a) shows the size dependence of the specific heat C for $J'/J = 0.025$ up to $L = 18$. In the figure, we can see the broad maximum of C of $L = 6$ around $T/J \sim 1.0$. At the same time, there emerges the small peak in the low temperature region, reflecting the 1D nature of the system. As L increases, this small peak rapidly merges into the broad peak coming down from the higher temperature side. We can then see that the merged peak rapidly develops into the sharp peak associated with the critical divergence at $T/J \sim 0.8$.

We next resolve the peak structure of the total specific heat by $C_{||}$, C_{\perp} and C_{cross} . Fig. 7(b) illustrates $C_{||}$, which exhibits the broad peak for small system size. Since $J \gg J'$, this broad peak can be attributed to the fluctuation of spins in the chain governed by the energy scale J . As L increases, the peak temperature shifts down toward $T \sim 0.8$ and the peak height itself increases in accordance with the criticality. On the other hand, C_{\perp} in Fig. 7(c) shows a clear finite size peak originating from the inter-chain fluctuation of the energy scale LJ' . As L increases, the peak temperature gradually increases from $T/J \sim 0.4$ toward 0.8. Then, an interesting point on C_{\perp} is that the shape of the peak is almost unchanged during shifting, in contrast to the 2D case where the peak considerably reduces its shape. Here, let us recall that, in sufficiently low temperature, the effective spins frozen in the chain direction form 2D network. Thus an important difference between 2D and 3D cases is that, for 3D, the effective 2D Ising model in the small J' limit can involve the quasi-critical divergence, while for 2D, the specific heat of the

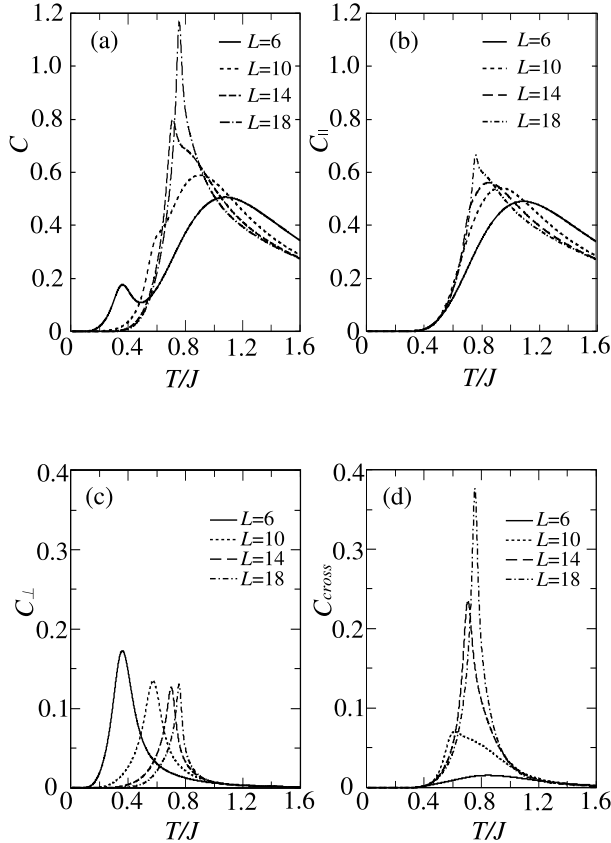


Fig. 7. C , $C_{||}$, C_{\perp} , and C_{cross} for the 3D Ising model of $J'/J = 0.025$

effective 1D Ising model does not show such divergence since there is no phase transition in the 1D Ising model. In Fig. 7(d), we finally present C_{cross} , the peak of which develops near T_c and is smoothly connected to the critical divergence.

In Fig. 8, we summarize the above size dependences of the peak temperatures for the specific heats. In the figure, the horizontal axis indicates the scaled system size $L^{-1/\nu}$, where we have used $\nu = 0.6301$.¹⁶ We can see that the round peak of $C_{||}$ comes down from the higher temperature side, but it still does not achieve the scaling region. On the other hand, we can see that C_{\perp} and C_{cross} are well fitted by linear functions, which are shown as the solid and broken lines in Fig.8. The straightforward extrapolation yields $T_c \simeq 0.85$, which is consistent with a precise estimation $T_c = 0.83$ based on the simulation up to the size $10 \times 10 \times 100$ (the result is not presented here). The similar analysis for the susceptibility was also reported in Ref.,⁸ where the peak temperature of the intra-chain spin fluctuation behaves similarly to C_{\perp} . The present result is consistent with this previous analysis of the susceptibility. As can be seen Fig. 7(a), the divergences of C_{cross} and C_{\perp} massively contribute to the critical divergence of the total specific heat C within the small system size. This suggests that C_{cross} can be expected to be suitable for finite size analysis of the critical behavior as well, although C exhibits rather complicated

size dependence of the peak structure in the 3D case. .

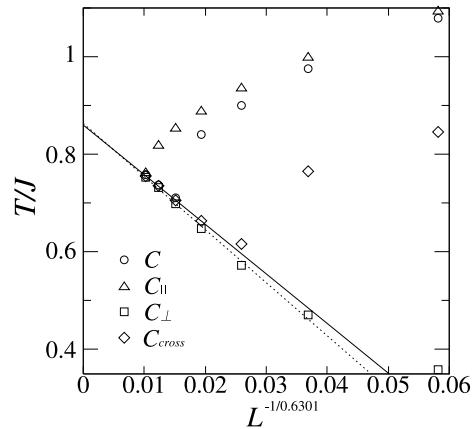


Fig. 8. The size dependences of the peak temperatures of C , $C_{||}$, C_{\perp} , and C_{cross} for the 3D Ising model of $J'/J = 0.025$. The scale of the horizontal axis follows $L^{-1/\nu}$ with $\nu = 0.6301$.¹⁶

4. Summary

We have studied the feature of the Q1D Ising model, using Wang-Landau simulation. In order to treat the difference of energy scale for the intra- and inter-chain directions, we have particularly introduced the two dimensional energy space $(e_{||}, e_{\perp})$ corresponding to the intra- and inter-chain directions. We further decomposed the total specific heat C as contributions from intra-chain fluctuation $C_{||}$, inter-chain fluctuation C_{\perp} , and cross term of the intra- and inter-chain fluctuation C_{cross} . Then the finite size effect peculiar to the Q1D system is discussed on the basis of the two dimensional DOS, and it was demonstrated that the chain flip configuration plays an essential role for the low temperature peak of the specific heat. We have also analyzed the shift exponent of the peak of the specific heat, and then found that C_{cross} can capture the critical behavior more effectively than the total specific heat C , within a relatively small system size. We have also discussed the qualitative difference between 2D and 3D cases in the low temperature and small J' limit; For 2D, the cross over of C_{\perp} from effective 1D chain to 2D model occurs rapidly around $L \sim J/J'$. While for 3D, the effective 2D Ising model itself involves the quasi-critical divergence, due to which C_{\perp} smoothly crossovers from the effective 2D model into the 3D critical behavior. Here, it should be recalled that the analytic contribution is non negligible for the analysis of the critical behavior of the specific heat for the isotropic 3D Ising model.¹⁹ As can be seen in Fig. 7, the complicated behavior of the total specific heat in the Q1D system might be adiabatically connected to such an analytic contribution in the isotropic case.

In this paper, we have analyzed the Q1D Ising model in the context of the two dimensional DOS. The actual computation cost to obtain the two dimensional DOS increases rapidly, as increasing system size, and then the

cluster algorithm seems to be more efficient for a simulation of a larger system. However, the present description based on the two dimensional DOS provides the essential insight for qualitative understanding of the low energy excitations in the Q1D system. In addition, for the purpose of suppressing the finite size effect peculiar to the Q1D system, the aspect ratio usually follows the ratio of the anisotropic correlation length in analyzing the critical behavior. We can also see that a possible aspect ratio of the system is $L'/L = (D - 1)J'/J$, where D is the dimension of the system, L is the length of a chain and L' is the size of the inter-chain directions. This is because the scale of the single spin flip excitation and the chain flipped state can be of the same order $4J + 4(D - 1)J' \simeq 4(D - 1)J'L$ for $J \gg J'$.

Acknowledgment

This work is supported by Grants-in-Aid for Scientific Research from the Ministry of Education, Culture, Sports, Science and Technology of Japan (No. 18740230 and No20340096), and by a Grant-in-Aid for Scientific Research on Priority Area "High-field spin science in 100T". One of the authors(K.O.) would like to thank T. Suzuki and M. Kikuchi for valuable discussions.

1) L.J. de Jongh, A.R. Miedem: Adv. Phys. **23** (1974) 1.

2) I. Tsukada, Y. Sasago, K. Uchinokura, A. Zheludev, S. Maslov, G. Shirane, K. Kakurai, and E. Ressouche, Phys. Rev. B **60**,

(1999) 6601.

- 3) S. Kimura, T. Takeuchi, K. Okunishi, M. Hagiwara, Z. He, K. Kindo, T. Taniyama, M. Itoh: Phys. Rev. Lett. **100**,(2008) 057202, S. Kimura, M. Matsuda, T. Masuda, S. Hondo, K. Kaneko, N. Metoki, M. Hagiwara, T. Takeuchi, K. Okunishi, Z. He, K. Kindo, T. Taniyama, M. Itoh: Phys. Rev. Lett. **101**, (2008) 207201.
- 4) K. Okunishi and T. Suzuki: Phys. Rev. B **76** (2007) 224411., T. Suzuki, N. Kawashima and K. Okunishi: J. Phys. Soc. Jpn. **76**, (2007) 123707
- 5) C. Y. Weng, R. B. Griffiths and M. E. Fisher: Phys. Rev. 162 (1967)475.; M. E. Fisher: Phys. Rev. 162 (1967) 480.
- 6) L. L. Liu and H. E. Stanley, Phys. Rev. Lett. **29**, 927 (1972); L. L. Liu and H. E. Stanley, Phys. Rev. B **8**, 2279 (1973).
- 7) T. Graim and D.P. Landau: Phys. Rev. B **24** (1981) 5156.
- 8) K. W. Lee: J. Phys. Soc. Jpn. **71** (2002) 2591
- 9) S. Todo: Phys. Rev. B. **74** (2006) 104415.
- 10) T. Nakamura: Phys. Rev. Lett. **101**, (2008) 210602.
- 11) F. Wang and D. P. Landau: Phys. Rev. Lett. **86** (2001) 2050.
- 12) F. Wang and D. P. Landau: Phys. Rev. E. **64** (2001) 056101.
- 13) H. K. Lee, Y. Okabe and D. P. Landau: Bull. Comput. Phys. Commun. **175** (2006) 36.
- 14) C. Zhou and R. N. Bhatt: Phys. Rev. E. **72** (2005) 025701(R).
- 15) L. H. Onsager, Phys. Rev. **65**, 117 (1944).
- 16) H. W. J. Blöte, E. Luijten and J. R. Heringa: J. Phys. A **28** (1995) 6289
- 17) In order to extract the proper critical behavior, the aspect ratio of the system may be adjusted to the Q1D system. In this paper, however, we discuss the size dependence within the square or cubic shaped systems.
- 18) K. Binder and J-S Wang, J. Stat. Phys **55** (1989) 87. See also Ref.⁷
- 19) M Hasenbusch and K Pinn: J. Phys. A: Math. Gen. **31**, (1998) 6157